Micro shape control, riblets and drag minimization

Matthieu Bonnivard Dorin Bucur

Abstract

Relying on the rugosity effect, we analyse the drag minimization problem in relation with the micro-structure of the surface of a given obstacle. We construct a mathematical framework for the optimization problem, prove the existence of an optimal solution by Γ-convergence arguments and analyse the stability of the drag with respect to the micro-structure. For Stokes flows we justify why rugosity increases the drag, while for Navier-Stokes flows we give some numerical evidence supporting the thesis that adding rugosity on specific regions of the obstacle may contribute to decrease the drag.

Keywords: drag minimization, rugosity effect, micro-shape control

1 Introduction

The main purpose of the paper is to analyse the drag minimization problem in relation with the micro-structure on the surface of a shape. The minimization of the drag with respect to the shape is a debated question. Given a model for the fluid motion and a contact law (e.g. stationary Navier Stokes equations with no-slip conditions), the question of optimizing the shape in order to minimize the drag may be answered in the classical framework of shape optimization problems (see [7], [10], [12], [14], [17], [19], [22]). In this paper, the drag minimization problem is discussed from a different point of view. Our problem is the following: given a fixed shape S and a non perfectly adherent material, the purpose is to create a microscopic structure on the surface of the shape such that the drag diminishes. We set the problem in terms of the rugosity effect relying on the friction-driven boundary conditions introduced in [4] and prove the existence of a solution which, loosely speaking, may be approached by a family of riblets with rough bottoms.

It is commonly accepted that rough surfaces *increase* the drag. From a mathematical point of view, this is true provided one deals with fluids obeying to Stokes equations (see Section 3). In the context of Navier-Stokes flows, it was noticed that contrary to this reasonable observation, the drag may decrease in contact with rough surfaces. In this paper, we intend to give a mathematical formulation to this micro-shape optimization problem, to analyse the question of the existence of an optimal micro-structure and to provide some numerical computations supporting our observations.

Our fundamental hypothesis is that the contact law between the fluid and the obstacle is of Navier type. From a physical point of view, this assumption may be justified by recent experimental studies that have measured significant slip lengths in the vicinity of a solid boundary in the context of microfluidics (see [15, 20, 21]). Formally, the Navier conditions

on the boundary of the obstacle read (see also the general formulation in relation (6) below and the comments thereafter)

$$\mathbf{u} \cdot \mathbf{n} = 0, [2\nu \mathbf{D}(\mathbf{u})\mathbf{n}]_{tan} + \beta \mathbf{u} = 0,$$

where $\mathbf{u}$ is the velocity of the fluid, $\mathbf{n}$ the outward normal field at the boundary of the obstacle, μ the viscosity and β the friction coefficient. The perfect adherence (*no-slip* condition) corresponds formally to $\beta = +\infty$. Roughly speaking, in this paper we prove that as soon as the material is not perfectly adherent (i.e. $\beta < +\infty$), the rugosity may play a role in the drag minimization problem. A micro-structure on such a slippery material may *significantly* influence the solutions of the Navier-Stokes equations, and consequently the drag. On the contrary, creating a micro-structure (riblets, denticles, etc.) on *perfectly adherent* material will produce a non significant variation of the drag, since the variations of the solution of the Navier-Stokes equations are small. Experimental observations of this mathematical result are listed in [23].

We assume in this paper that the (macro) shape of the obstacle is fixed and that the material is not perfectly adherent (the friction coefficient $\beta < +\infty$ is fixed). We consider an ideal perfectly slippery material for setting our theoretical framework, while for the numerical experiments we choose different values for β. For a given β, the control space is the family of *micro-structures* on the surface of the material. The micro-structures have as effect the modification of the contact law and, from a mathematical point of view, they are the boundary conditions of friction-driven type resulting from the asymptotic behaviour of the rugosities on the surface of the material (see [4] and Theorem 2.1 below). We study the influence of the micro-structure on the drag and analyse the drag minimization problem with respect to the micro-structure for both Stokes and stationary Navier-Stokes equations. We prove that for Stokes equations, the drag satisfies a certain monotonicity property with respect to the micro-structure, so that riblets cannot be used to diminish the drag of an obstacle in a Stokes flow. On the contrary, for Navier-Stokes equations the drag is not anymore monotone, and we exhibit some numerical evidence showing that adding rugosity may decrease the drag.

Although we are not able to give a full answer to the optimization problem, the main objectives of the paper are:

- to introduce a mathematical framework for the drag minimization problem with respect to the micro-structure of the surface. For this purpose, we develop a Γ-convergence framework and study the drag as a function of the micro-structure;
- to prove that for Navier-Stokes equations the problem is well-posed and admits a solution in terms of friction-driven boundary conditions;
- to show that for Stokes equations, rugosity increases the drag;
- to perform numerical computations which support our mathematical results. We justify the optimization approach and confirm the non-monotonicity of the drag with respect to the friction-driven boundary conditions for Navier-Stokes equations;

- to give an example of complex rugosity effect modeled by combinations of perfectly slippery regions with in-flow micro perforations.

The structure of the paper is the following. In Section 2, we introduce the mathematical approach of the rugosity effect and recall the main results of [4]. In Section 3, we develop the mathematical framework for the drag minimization, prove the existence of a solution and discuss the monotonicity of the drag with respect to the micro-structures. We prove that monotonicity holds (only) for the Stokes equation, while the non-variational character of the Navier-Stokes equations leads to lack of monotonicity and, as a consequence, justifies the well-posedness of the optimization problem. In Section 4, we perform numerical computations for the Navier-Stokes equation to support the non-monotonicity argument and to justify the optimization framework. Section 5 is devoted to an example of complex rugosity effect which falls out of the friction-driven boundary conditions. This example shows that a modification of the contact law on asymptotically small regions may lead to a macroscopic effect on the flow, and significantly enlarges the class of admissible controls.

2 The rugosity effect: a mathematical approach

Throughout the paper, by ε we denote a generic sequential parameter which converges to 0. By $B_r(x)$ we denote the open ball of $\mathbb{R}^N$, centred at x and of radius r.

Capacitary measures. Let $\Omega \subseteq \mathbb{R}^N$ be a bounded open set. The capacity of a subset E in Ω is

$$\mathrm{cap}(E,\Omega) = \inf\Big\{ \int_\Omega |\nabla u|^2 \,\mathrm{d}x \,:\, u \in \mathcal{U}_E \Big\}\,,$$

where $\mathcal{U}_E$ is the set of all functions u of the Sobolev space $H^1_0(\Omega)$ such that $u \geq 1$ almost everywhere in a neighborhood of E.

If a property $P(x)$ holds for all $x \in E$ except for the elements of a set $Z \subseteq E$ with $\mathrm{cap}(Z,\Omega) = 0$, we say that $P(x)$ holds *quasi-everywhere* on E (shortly *q.e.* on E). The expression *almost everywhere* (shortly *a.e.*) refers, as usual, to the Lebesgue measure. A subset A of Ω is said to be *quasi-open* if for every $\varepsilon > 0$ there exists an open subset A_ε of Ω, such that $A \subseteq A_\varepsilon$ and $\mathrm{cap}(A_\varepsilon \setminus A, \Omega) < \varepsilon$. A function $f\colon \Omega \to \mathbb{R}$ is said to be *quasi-continuous* if for every $\varepsilon > 0$ there exists a continuous function $f_\varepsilon\colon \Omega \to \mathbb{R}$ such that $\mathrm{cap}(\{f \neq f_\varepsilon\}, \Omega) < \varepsilon$, where $\{f \neq f_\varepsilon\} = \{x \in \Omega : f(x) \neq f_\varepsilon(x)\}$. It is well known (see, e.g., Ziemer [24]) that every function u of the Sobolev space $H^1(\Omega)$ has a quasi-continuous representative, which is uniquely defined up to a set of capacity zero. We shall always identify the function u with its quasi-continuous representative, so that a pointwise condition can be imposed on $u(x)$ for quasi-every $x \in \Omega$.

We denote by $\mathcal{M}_0(\Omega)$ the set of all nonnegative Borel measures μ on Ω, possibly $+\infty$ valued, such that

i) $\mu(B) = 0$ for every Borel set $B \subseteq \Omega$ with $\mathrm{cap}(B,\Omega) = 0$,

ii) $\mu(B) = \inf\{\mu(U) : U \text{ quasi-open},\ B \subseteq U\}$ for every Borel set $B \subseteq \Omega$.

We stress the fact that the measures $\mu \in \mathcal{M}_0(\Omega)$ do not need to be finite, and may take the value $+\infty$ even on large parts of Ω.

Given an arbitrary subset E of Ω, we denote by $\infty|_E$ the measure defined by

i) $\infty|_E(B) = 0$ for every Borel set $B \subseteq \Omega$ with $\mathrm{cap}(B \cap E, \Omega) = 0$,

ii) $\infty|_E(B) = +\infty$ for every Borel set $B \subseteq \Omega$ with $\mathrm{cap}(B \cap E, \Omega) > 0$.

For a quasi-open set $A \subseteq \Omega$, we always identify A with the measure $\infty|_{\Omega\setminus A}$ and observe that $H^1_0(\Omega) \cap L^2(\Omega, \infty|_{\Omega\setminus A}) = H^1_0(A)$ (see [11, 3]).

Navier-Stokes equations with friction-driven boundary conditions. Let S be a closed Lipschitz subset of a smooth bounded open set $\Omega \subseteq \mathbb{R}^3$. In the sequel, we will consider only measures $\mu \in \mathcal{M}_0(\Omega)$ which are supported on ∂S. In particular, if $\mu \not\equiv 0$, then its support cannot be contained in a one dimensional smooth subset of ∂S since this set has zero capacity.

We consider a family of linear spaces $\mathcal{V} := \{V(x)\}_{x\in\partial S}$, where $V(x)$ is a subspace of the tangent hyperplane (where it exists) at $x \in \partial S$. In particular, the dimension of $V(x)$ does not exceed 2. Furthermore, let $a_{i,j} : \partial S \to \mathbb{R}$, $1 \le i, j \le 3$, be Borel functions such that $a_{i,j} = a_{j,i}$, and $\sum_{i,j=1}^3 a_{ij}\xi_i\xi_j \ge 0$ for all $\xi \in \mathbb{R}^3$. We set $A = \{a_{i,j}\}_{i,j=1}^3$. We also consider a constant vector field $\mathbf{u}_\infty \in \mathbb{R}^3$.

Following [4], the Navier-Stokes problem with friction-driven boundary conditions reads: find $(\mathbf{u}, p) \in \mathbf{H}^1(\Omega \setminus S) \times L^2(\Omega \setminus S)$ such that

$$-\mathrm{div}\ \sigma(\mathbf{u}, p) + (\mathbf{u}\cdot\nabla)\mathbf{u} = 0 \text{ in } \Omega \setminus S, \tag{1}$$

$$\mathrm{div}\ \mathbf{u} = 0 \text{ in } \Omega \setminus S, \tag{2}$$

$$\mathbf{u} = \mathbf{u}_\infty \text{ on } \partial\Omega, \tag{3}$$

$$\mathbf{u}(x) \in V(x) \text{ for q.e. } x \in \partial S, \tag{4}$$

$$\Big[2\nu\mathbf{D}(\mathbf{u})\mathbf{n} + \mu A\mathbf{u}\Big] \cdot \mathbf{v} = 0 \text{ for } \mathbf{v} \in V(x), \text{ q.e. } x \in \partial S, \tag{5}$$

where $\sigma(\mathbf{u}, p)$ is the stress tensor defined by

$$\sigma(\mathbf{u}, p) = 2\nu\mathbf{D}(\mathbf{u}) - p\mathrm{Id},$$

$\mathbf{D}(\mathbf{u})$ being the symmetric part of $\nabla\mathbf{u}$ defined by

$$\mathbf{D}(\mathbf{u}) = \frac{1}{2}\left((\nabla\mathbf{u}) + (\nabla\mathbf{u})^T\right).$$

Above, $\Big[2\nu\mathbf{D}(\mathbf{u})\cdot\mathbf{n} + \mu A\mathbf{u}\Big] \cdot \mathbf{v} = 0$ for $\mathbf{v} \in V(x)$, is a formal q.e. pointwise relation, which has to be understood globally on ∂S *via* the weak form of the equation. Precisely, we say that $(\mathbf{u}, p) \in \mathbf{H}^1(\Omega \setminus S) \times L^2(\Omega \setminus S)$ is a weak solution to System (1)-(5) provided that $\mathbf{u} \in H^1(\Omega \setminus S, \mathbb{R}^3)$ is such that $\mathrm{div}\ \mathbf{u} = 0$ in $\Omega \setminus S$, $\mathbf{u}(x) \in V(x)$ for q.e. $x \in \partial S$, $\mathbf{u}(x) = \mathbf{u}_\infty$ on $\partial\Omega$, and satisfies

$$2\nu\int_{\Omega\setminus S} \mathbf{D}(\mathbf{u}) : \mathbf{D}(\phi)\ \mathrm{d}x + \int_{\Omega\setminus S} [(\mathbf{u}\cdot\nabla)\mathbf{u}]\cdot\phi\ \mathrm{d}x + \int_{\partial S} A\mathbf{u}\cdot\phi\ d\mu = 0, \tag{6}$$

for every $\phi \in \mathbf{H}^1(\Omega \setminus S)$ such that div $\phi = 0$ in $\Omega \setminus S$, $\phi(x) \in V(x)$ for q.e. $x \in \partial S$, $\int_{\partial S} A\phi \cdot \phi \, d\mu < +\infty$ and $\phi(x) = 0$ on $\partial\Omega$. The "classical" Navier boundary conditions occur in the situation in which $A \equiv \mathrm{Id}$, $\mu \equiv \beta \mathcal{H}^2\lfloor_{\partial S}$ and for q.e. $x \in \partial S, V(x) = \mathbb{R}^2$. In our framework, $\mathbf{u}_\infty$ is a constant vector field representing the velocity of the fluid at infinity.

Notice that if $\mu \equiv 0$ and for q.e. $x \in \partial S, V(x) = \mathbb{R}^2$, then the friction-driven boundary conditions are precisely the perfect slip ones (the choice of A is not important in this case). If $A \equiv \mathrm{Id}$, $\mu = +\infty|_{\partial S}$ and V is arbitrary, or, alternatively, if A and μ are arbitrary but for q.e. $x \in \partial S$, $V(x) = \{0\}$, then the boundary conditions correspond to the no-slip condition.

The rugosity effect. We consider a sequence S_ε of equi-Lipschitz closed sets, converging to $S \subset \Omega$ in the Hausdorff metric, i.e.

$$d(\cdot, S_\varepsilon) \to d(\cdot, S) \text{ uniformly on } \Omega, \tag{7}$$

where $d(\cdot, F)$ denotes the distance function to the set F.

The main result of [4] reads as follows.

Theorem 2.1 *Let $\varepsilon \to 0$ and $\{\mathbf{u}_\varepsilon\}_{\varepsilon>0}$ be a family of (weak) solutions to Navier-Stokes equations* (1)-(5) *in $\Omega \setminus S_\varepsilon$ with perfect slip conditions on ∂S_ε, such that $\exists M > 0 \ \forall \varepsilon > 0, \|\mathbf{u}_\varepsilon\|_{\mathbf{H}^1(\Omega\setminus S_\varepsilon)} \leq M$. Then, at least for a suitable subsequence,*

$$1_{\Omega\setminus S_\varepsilon}\mathbf{u}_\varepsilon \to 1_{\Omega\setminus S}\mathbf{u} \text{ (strongly) in } L^2(\mathbb{R}^3, \mathbb{R}^3),$$

$$1_{\Omega\setminus S_\varepsilon}\nabla\mathbf{u}_\varepsilon \rightharpoonup 1_{\Omega\setminus S}\nabla\mathbf{u} \text{ weakly in } L^2(\mathbb{R}^3, \mathbb{R}^{3\times 3}),$$

and there exists a suitable triplet $\{\mu, A, \mathcal{V}\}$ such that $\mathbf{u}$ is a solution in $\Omega \setminus S$ to Navier-Stokes equations with friction-driven boundary conditions (1)-(5).

We underline the fact that the triplet $\{\mu, A, \mathcal{V}\}$ is of geometric nature, being independent both on Ω and $\mathbf{u}_\infty$. By abuse of language, we call *micro-structure* on the boundary of S a triplet $\{\mu, A, \mathcal{V}\}|_{\partial S}$.

3 Drag minimization with respect to the micro-structure

In a first step, we introduce the family of admissible micro-structures. We fix an angle $\pi/2 > \theta > 0$ and we work with obstacles S which are closed subsets of Ω satisfying the θ-cone condition (see [12, Definition 2.4.1] and [12, Theorem 2.4.7]). More specifically, let

$$C(x, \theta, \xi) = \{y \in \mathbb{R}^N : |y - x| < \theta, (y - x, \xi) \geq \cos(\theta)|y - x|\}$$

be the cone with vertex at x, aperture 2θ, height θ, and orientation given by a unit vector ξ. We say that S satisfies the θ-cone condition if for any $x_0 \in \partial S$, there exists a unit vector $\xi_{x_0} \in \mathbb{R}^N$ such that

$$C(x, \theta, \xi_{x_0}) \subseteq \Omega \setminus S \text{ whenever } x \in B(x_0, \theta) \cap \overline{\Omega \setminus S}.$$

We recall that if S_ε converges to S in the Hausdorff metric and all of them satisfy the θ-cone condition, then

$$1_{S_\varepsilon} \to 1_S \text{ in } L^1(\Omega) \text{ as } \varepsilon \to 0. \tag{8}$$

Definition 3.1 *Let $(S_\varepsilon)_\varepsilon$ be a sequence of closed subsets of Ω satisfying the θ-cone condition. Assume S_ε converges in the Hausdorff metric to a closed set $S \subseteq \Omega$. Let $\{\mu_\varepsilon, A_\varepsilon, \mathcal{V}_\varepsilon\}|_{\partial S_\varepsilon}$ be a micro-structure on ∂S_ε. We say that $\{\mu_\varepsilon, A_\varepsilon, \mathcal{V}_\varepsilon\}|_{\partial S_\varepsilon}$ γ-converges to $\{\mu, A, \mathcal{V}\}|_{\partial S}$ if the functionals*

$$F_\varepsilon(\mathbf{v}) = \begin{cases} 2\nu \displaystyle\int_{\Omega\setminus S_\varepsilon} |\mathbf{D}(\mathbf{v})|^2 \mathrm{d}x + \int_{\partial S_\varepsilon} A_\varepsilon \mathbf{v}\cdot\mathbf{v}\mathrm{d}\mu_\varepsilon & \text{if } \mathbf{v}\in H^1_0(\Omega,\mathbb{R}^3),\ \mathrm{div}\ \mathbf{v}=0 \text{ in } \Omega\setminus S_\varepsilon, \\ & \mathbf{v}(x)\in V_\varepsilon(x), \text{q.e. } x\in\partial S_\varepsilon, \\ +\infty & \text{otherwise,} \end{cases} \tag{9}$$

Γ-converges to F in $L^2(\Omega,\mathbb{R}^3)$, where

$$F(\mathbf{v}) = \begin{cases} 2\nu \displaystyle\int_{\Omega\setminus S} |\mathbf{D}(\mathbf{v})|^2 \mathrm{d}x + \int_{\partial S} A\mathbf{v}\cdot\mathbf{v}\mathrm{d}\mu & \text{if } \mathbf{v}\in H^1_0(\Omega,\mathbb{R}^3),\ \mathrm{div}\ \mathbf{v}=0 \text{ in } \Omega\setminus S, \\ & \mathbf{v}(x)\in V(x), \text{q.e. } x\in\partial S, \\ +\infty & \text{otherwise.} \end{cases} \tag{10}$$

We briefly recall that a sequence of functionals $F_\varepsilon : L^2(\Omega,\mathbb{R}^3) \to \mathbb{R}\cup\{+\infty\}$ Γ-converges to F in $L^2(\Omega,\mathbb{R}^3)$ if

$$\forall \mathbf{v}_\varepsilon \to \mathbf{v} \text{ in } L^2(\Omega,\mathbb{R}^3) \Longrightarrow F(\mathbf{v}) \le \liminf_{\varepsilon\to 0} F_\varepsilon(\mathbf{v}_\varepsilon),$$

$$\forall \mathbf{v}\in L^2(\Omega,\mathbb{R}^3), \exists \mathbf{v}_\varepsilon \to \mathbf{v} \text{ in } L^2(\Omega,\mathbb{R}^3) \text{ such that } F(\mathbf{v}) \ge \limsup_{\varepsilon\to 0} F_\varepsilon(\mathbf{v}_\varepsilon).$$

For details on the Γ-convergence, we refer the reader to [6]. As usual, in optimal control theory, in the definition above we denote by Γ the classical *Gamma convergence* of functionals and by γ the topology induced on the space of controls (here the micro-structures).

A micro-structure $\{\mu, A, \mathcal{V}\}|_{\partial S}$ is admissible on S as soon as it is obtained through the rugosity effect, i.e. is a γ-limit obtained from a sequence (S_ε) which satisfies the θ-cone condition, in the frame of Theorem 2.1. For every $\beta\in[0,+\infty)$, we introduce

$$\mathcal{U}_\beta = \Big\{ \{\mu, A, \mathcal{V}\}|_{\partial S} : \exists S_\varepsilon \to S \ \text{ such that } \{\beta\mathcal{H}^2|_{\partial S_\varepsilon}, \mathrm{Id}, \mathbb{R}^2\}|_{\partial S_\varepsilon} \xrightarrow{\gamma} \{\mu, A, \mathcal{V}\}|_{\partial S} \Big\}.$$

We refer to the recent paper [5, Theorem 3.4], where explicit constructions of periodic-like rugosity lead to an augmentation of the friction coefficient for flat boundaries. As a consequence of this result, one could prove that for polyhedral obstacles and for every friction coefficients $\beta > \beta' \ge 0$, the family $\mathcal{U}_\beta$ is a subclass of $\mathcal{U}_{\beta'}$. Extending this result to general Lipschitz obstacles requires some technicalities related to the approximation result of Lipschitz domains by C^2 domains, due to Nečas [18]. This fact is not necessary for our considerations.

Remark 3.2 Let us notice that the definition above implies the continuity of the solutions to Stokes equations with respect to the γ-convergence of the micro-structures. Indeed, let us consider Stokes equations in $\Omega \setminus S$ with friction-driven boundary conditions $\{\mu, A, \mathcal{V}\}|_{\partial S}$, i.e.

$$-\text{div } \sigma(\mathbf{u}, p) = 0 \text{ in } \Omega \setminus S, \tag{11}$$

$$\text{div } \mathbf{u} = 0 \text{ in } \Omega \setminus S, \tag{12}$$

$$\mathbf{u} = \mathbf{u}_\infty \text{ on } \partial\Omega, \tag{13}$$

$$\mathbf{u}(x) \in V(x) \text{ for q.e. } x \in \partial S, \tag{14}$$

$$\Big[2\nu \mathbf{D}(\mathbf{u})\mathbf{n} + \mu A\mathbf{u}\Big] \cdot \mathbf{v} = 0 \text{ for } \mathbf{v} \in V(x),\ x \in \partial S. \tag{15}$$

The weak solution $\mathbf{u}$ to System (11)-(15) is also the unique minimizer of

$$H(\mathbf{v}) := 2\nu \int_{\Omega\setminus S} |\mathbf{D}(\mathbf{v})|^2 \mathrm{d}x + \int_{\partial S} A\mathbf{v} \cdot \mathbf{v} \mathrm{d}\mu, \tag{16}$$

over

$$\mathcal{C} := \ \Big\{ \mathbf{v} \in H^1(\Omega, \mathbb{R}^3) \ \Big|\ \text{div } \mathbf{v} = 0 \text{ in } \Omega,\ \mathbf{v}(x) \in V(x) \text{ for q.e. } x \in \partial S, \mathbf{v} = \mathbf{u}_\infty \text{ on } \partial\Omega \Big\}.$$

As $\mathcal{C}$ is a closed subspace of $H^1(\Omega \setminus S, \mathbb{R}^3)$, the classical Lax-Milgram theorem together with Korn's inequality give existence and uniqueness of the solution.

Assume now that $(S_\varepsilon)_\varepsilon$ satisfies the assumptions of Definition 3.1 and denote by $\mathbf{u}_\varepsilon$ the solution to Equations (11)-(15) on $\Omega \setminus S_\varepsilon$ with boundary conditions $\{\mu_\varepsilon, A_\varepsilon, \mathcal{V}_\varepsilon\}$. Let $\eta \in C^\infty(\overline{\Omega})$ be a function equal to 1 on $\partial\Omega$ and to 0 on a neighbourhood of S. Observe that for every $\mathbf{v} \in H^1(\Omega, \mathbb{R}^3)$ such that $\mathbf{v} = \mathbf{u}_\infty$ on $\partial\Omega$,

$$H_\varepsilon(\mathbf{v}) = F_\varepsilon(\mathbf{v} - \eta\mathbf{u}_\infty) - 4\nu \int_{\Omega\setminus S_\varepsilon} \mathbf{D}(\mathbf{v}) : \mathbf{D}(\eta\mathbf{u}_\infty)\mathrm{d}x + 2\nu \int_{\Omega\setminus S_\varepsilon} |\mathbf{D}(\eta\mathbf{u}_\infty)|^2 \mathrm{d}x.$$

Consequently, H_ε Γ-converges in $L^2(\Omega, \mathbb{R}^3)$ to H, thus their minimizers also converge in $L^2(\Omega, \mathbb{R}^3)$.

Remark 3.3 In the language of γ-convergence, Theorem 2.1 asserts that for the sequence of obstacles S_ε which converges to S in the Hausdorff metric, the associated micro-structures $\{0, \mathrm{Id}, \mathbb{R}^2\}|_{\partial S_\varepsilon}$ γ-converge to$\{\mu, A, \mathcal{V}\}|_{\partial S}$. In fact, Remark 3.2 is an extension of Theorem 2.1. As well, we emphasize that the geometric effect of the rugosity is the same on both Stokes and Navier-Stokes equations, in the sense that if $\{\mu_\varepsilon, A_\varepsilon, \mathcal{V}_\varepsilon\}|_{\partial S_\varepsilon}$ γ-converges to $\{\mu, A, \mathcal{V}\}|_{\partial S}$, the solutions to Navier-Stokes equations (1)-(5) on $\Omega \setminus S_\varepsilon$ with friction-driven boundary conditions $\{\mu_\varepsilon, A_\varepsilon, \mathcal{V}_\varepsilon\}$ converge as in Theorem 2.1. The argument is similar to [4, Remark 4.4 and Theorem 5.1] and relies on the persistence of the Γ-convergence for continuous perturbations.

Remark 3.4 The topology of the γ-convergence is metrizable and compact in the family of micro-stuctures associated to obstacles satisfying a θ-cone conditions and which are contained in a compact subset of Ω. Metrizability is a consequence of the equi-coerciveness of the functionals F_ε and of the separability of $L^2(\Omega)$ (see [6, Theorem 10.22]), and compactness is a consequence of the main result in [4].

Theorem 3.5 *For every $+\infty > \beta \geq 0$, the family $\mathcal{U}_\beta$, endowed with the topology of the γ-convergence, is compact.*

Proof. This is a consequence of Theorem 2.1, the metrizability of the γ-convergence and the definition by closure of $\mathcal{U}_\beta$. □

The result above is independent on the fact that for every $\beta > 0$, the Navier boundary condition with friction coefficient β can be obtained as the limit of oscillating boundaries with perfect slip condition. Of course, it would be very interesting to know, in general, whether for every obstacle and every $\beta' < \beta$ one has $\mathcal{U}_\beta \subseteq \mathcal{U}_{\beta'}$, but this is not necessary in our framework.

Let $\mathbf{u}$ be a solution to Navier Stokes (1)–(5), respectively Stokes (11)–(15), equations in $\Omega \setminus S$ with friction-driven boundary conditions. The drag function associated to the micro-structure and to $\mathbf{u}$ is given by the (same) formal expression

$$T(\{\mu, A, \mathcal{V}\}, \mathbf{u}) = 2\nu \int_{\partial S} |\mathbf{D}(\mathbf{u})|^2 \, \mathrm{d}x + \int_{\partial S} A\mathbf{u} \cdot \mathbf{u} \, \mathrm{d}\mu. \tag{17}$$

Remark 3.6 If $\mathbf{u}$ is a smooth solution to Navier Stokes equations (1)–(5) (or to Stokes equations (11)–(15)) in $\Omega \setminus S$, then the drag $T(\{\mu, A, \mathcal{V}\}, \mathbf{u})$ coincides with its physical expression, given by

$$\mathcal{T} = -\int_{\partial S} \sigma(\mathbf{u}, p)\mathbf{n} \cdot \mathbf{u}_\infty \, \mathrm{d}\mathcal{H}^2.$$

Indeed, we consider the case of stationary Navier-Stokes equations (Stokes system can be handled by dropping the inertial term $(\mathbf{u} \cdot \nabla)\mathbf{u}$ in the following computations). Assuming that $\mathbf{u}$ is smooth enough, Equation (1) yields the following identity in $L^2(\Omega \setminus S)$:

$$\mathrm{div}\ \sigma(\mathbf{u}, p) = (\mathbf{u} \cdot \nabla)\mathbf{u}.$$

Consequently,

$$\mathcal{T} = -\int_{\Omega \setminus S} [(\mathbf{u} \cdot \nabla)\mathbf{u}] \cdot \mathbf{u}_\infty \, \mathrm{d}\mathbf{x} + \int_{\partial\Omega} \sigma(\mathbf{u}, p)\mathbf{n} \cdot \mathbf{u}_\infty \, \mathrm{d}\mathcal{H}^2.$$

Using Green's formula and boundary condition (3), we express the boundary integral on $\partial\Omega$ as follows:

$$\int_{\partial\Omega} \sigma(\mathbf{u}, p)\mathbf{n} \cdot \mathbf{u}_\infty \, \mathrm{d}\mathcal{H}^2 = \int_{\Omega \setminus S} [(\mathbf{u} \cdot \nabla)\mathbf{u}] \cdot \mathbf{u} \, \mathrm{d}\mathbf{x} + \int_{\Omega \setminus S} \sigma(\mathbf{u}, p) : \mathbf{D}(\mathbf{u}) \, \mathrm{d}\mathbf{x} - \int_{\partial S} \sigma(\mathbf{u}, p)\mathbf{n} \cdot \mathbf{u} \, \mathrm{d}\mathcal{H}^2.$$

This yields the following expression of $\mathcal{T}$:

$$\mathcal{T} = \int_{\Omega \setminus S} [(\mathbf{u} \cdot \nabla)\mathbf{u}] \cdot (\mathbf{u} - \mathbf{u}_\infty) \, \mathrm{d}\mathbf{x} + \int_{\Omega \setminus S} \sigma(\mathbf{u}, p) : \mathbf{D}(\mathbf{u}) \mathrm{d}\mathbf{x} - \int_{\partial S} \sigma(\mathbf{u}, p)\mathbf{n} \cdot \mathbf{u} \, \mathrm{d}\mathcal{H}^2. \tag{18}$$

We only need to prove that the first integral vanishes. Indeed, using boundary condition (5) (in a strong pointwise sense),

$$\int_{\Omega \setminus S} \sigma(\mathbf{u}, p) : \mathbf{D}(\mathbf{u}) \, \mathrm{d}\mathbf{x} = 2\nu \int_{\Omega \setminus S} |\mathbf{D}(\mathbf{u})|^2 \, \mathrm{d}x,$$

and since $\mathbf{u}$ is solenoidal,

$$-\int_{\partial S}\sigma(\mathbf{u},p)\mathbf{n}\cdot\mathbf{u}\ \mathrm{d}\mathcal{H}^2=\int_{\partial\mathcal{S}}A\mathbf{u}\cdot\mathbf{u}\ \mathrm{d}\mu.$$

As well, since $\operatorname{div}\mathbf{u}=0$,

$$[(\mathbf{u}\cdot\nabla)\mathbf{u}]\cdot(\mathbf{u}-\mathbf{u}_\infty)=\frac{1}{2}\mathrm{div}\ \left(|\mathbf{u}-\mathbf{u}_\infty|^2\ \mathbf{u}\right),$$

and using Green's formula, we obtain

$$\int_{\Omega\setminus S}[(\mathbf{u}\cdot\nabla)\mathbf{u}]\cdot(\mathbf{u}-\mathbf{u}_\infty)\ \mathrm{d}\mathbf{x}=\frac{1}{2}\left(\int_{\partial S}|\mathbf{u}-\mathbf{u}_\infty|^2\ \mathbf{u}\cdot\mathbf{n}\ \mathrm{d}\mathcal{H}^2+\int_{\partial\Omega}|\mathbf{u}-\mathbf{u}_\infty|^2\ \mathbf{u}\cdot\mathbf{n}\ \mathrm{d}\mathcal{H}^2\right).$$

Relying on the non penetration condition on ∂S and boundary condition (3) on $\partial\Omega$, we get the desired result.

Theorem 3.7 *The drag is γ-continuous for the Stokes equations.*

Proof. Following Remark 3.2, the continuity of the drag for the γ-convergence is a direct consequence of the convergence of minima in the general framework of Γ-convergence. □

Since the solution to Navier-Stokes equations may not be unique, the assertion of Theorem 3.7 has to be modified as follows.

Theorem 3.8 *Assume that $\{\mu_\varepsilon,A_\varepsilon,\mathcal{V}_\varepsilon\}|_{\partial S_\varepsilon}\overset{\gamma}{\to}\{\mu,A,\mathcal{V}\}|_{\partial S}$. Let $(\mathbf{u}_\varepsilon)$ be a family of weak solutions to Navier-Stokes equations with friction-driven boundary conditions $\{\mu_\varepsilon,A_\varepsilon,\mathcal{V}_\varepsilon\}$ on S_ε. If $\sup_\varepsilon T(\{\mu_\varepsilon,A_\varepsilon,\mathcal{V}_\varepsilon\},\mathbf{u}_\varepsilon)<+\infty$, then there exists a solution $\mathbf{u}$ to Navier-Stokes equations (1)-(5) on $\Omega\setminus S$ and a subsequence (still denoted using the same index) such that*

$$T(\{\mu_\varepsilon,A_\varepsilon,\mathcal{V}_\varepsilon\},\mathbf{u}_\varepsilon)\to T(\{\mu,A,\mathcal{V}\},\mathbf{u}).$$

Proof. Indeed, since $\sup_\varepsilon T(\{\mu_\varepsilon,A_\varepsilon,\mathcal{V}_\varepsilon\},\mathbf{u}_\varepsilon)<+\infty$, we can assume that $\sup_\varepsilon\|\tilde{\mathbf{u}}_\varepsilon\|_{H^1(\Omega,\mathbb{R}^3)}<+\infty$, where $\tilde{\mathbf{u}}_\varepsilon$ are suitable extensions of $\mathbf{u}_\varepsilon$ on S_ε. Consequently, there exists a second subsequence (still denoted with the same index) such that $\mathbf{u}_\varepsilon\rightharpoonup\mathbf{u}$ weakly in $H^1(\Omega,\mathbb{R}^3)$. In particular,

$$1_{\Omega\setminus S_\varepsilon}\mathbf{u}_\varepsilon\to 1_{\Omega\setminus S}\mathbf{u}\ \text{(strongly) in}\ L^2(\mathbb{R}^3,\mathbb{R}^3),\tag{19}$$

$$1_{\Omega\setminus S_\varepsilon}\nabla\mathbf{u}_\varepsilon\rightharpoonup 1_{\Omega\setminus S}\nabla\mathbf{u}\ \text{weakly in}\ L^2(\mathbb{R}^3,\mathbb{R}^{3\times3}).\tag{20}$$

We define $f_\varepsilon=-1_{\Omega\setminus S_\varepsilon}(\mathbf{u}_\varepsilon\cdot\nabla)\mathbf{u}_\varepsilon\in H^{-1}(\Omega,\mathbb{R}^3)$, and notice that $f_\varepsilon\to f:=-1_{\Omega\setminus S}(\mathbf{u}\cdot\nabla)\mathbf{u}$ strongly in $H^{-1}(\Omega,\mathbb{R}^3)$.

Since $H_\varepsilon\overset{\Gamma}{\longrightarrow}H$, we observe that

$$\frac{1}{2}H_\varepsilon(\cdot)-<f_\varepsilon,\cdot>_{H^{-1}(\Omega)\times H_0^1(\Omega)}\overset{\Gamma}{\longrightarrow}\frac{1}{2}H(\cdot)-<f,\cdot>_{H^{-1}(\Omega)\times H_0^1(\Omega)}.$$

Since $\mathbf{u}_\varepsilon$ are minimizers of the modified functionals and they converge to $\mathbf{u}$ in the sense (19)-(20), we get that $\mathbf{u}$ is a minimizer of $\frac{1}{2}H(\cdot)-<f,\cdot>_{H^{-1}(\Omega)\times H_0^1(\Omega)}$. As a result, $\mathbf{u}$ is

a solution to Navier-Stokes equations, since it satisfies the Euler equation associated to a minimizer.

For the function η defined in Remark 3.2, taking $\mathbf{u}_\varepsilon - \eta\mathbf{u}_\infty$ and $\mathbf{u} - \eta\mathbf{u}_\infty$ as test functions in the respective Euler equations, we get that

$$T(\{\mu_\varepsilon, A_\varepsilon, \mathcal{V}_\varepsilon\}, \mathbf{u}_\varepsilon) =$$
$$2\nu \int_{\Omega\setminus S_\varepsilon} \mathbf{D}(\mathbf{u}_\varepsilon) : \mathbf{D}(\eta\mathbf{u}_\infty)\mathrm{d}x + \int_{\partial S_\varepsilon} A_\varepsilon \mathbf{u}_\varepsilon \cdot (\eta\mathbf{u}_\infty)\mathrm{d}\mu_\varepsilon + < f_\varepsilon, \mathbf{u}_\varepsilon - \eta\mathbf{u}_\infty >_{H^{-1}(\Omega)\times H^1_0(\Omega)} .$$

The right hand side passes to the limit since $\mathbf{u}_\varepsilon$ converges weakly in $H^1(\Omega, \mathbb{R}^3)$, the boundary term $\int_{\partial S_\varepsilon} A_\varepsilon \mathbf{u}_\varepsilon \cdot (\eta\mathbf{u}_\infty)\mathrm{d}\mu_\varepsilon$ vanishes and $f_\varepsilon \to f$ strongly in $H^{-1}(\Omega, \mathbb{R}^3)$. □

Theorems 3.7 and 3.8 provide two pieces of information. The first one is practical: the drag associated to friction-driven boundary conditions is close to the drag associated to rugous domains. Consequently, optimal friction-driven boundary conditions can be approached by rugous domains. Second, from a mathematical point of view, if two micro-structures are close in the γ-distance, the associated drags are also close.

Corollary 3.9 *For every $+\infty > \beta \geq 0$, the drag minimization problem on $\mathcal{U}_\beta$ for Stokes, respectively Navier-Stokes, equations has at least one solution.*

Proof. This is a direct consequence of Theorems 3.5 and 3.7 (respectively 3.8). □

Drag monotonicity for Stokes equations. We consider Stokes equations with friction-driven boundary conditions (11)-(15) associated to a fixed obstacle S and different micro-structures $\{\mu, A, \mathcal{V}\}|_{\partial S}$.

Theorem 3.10 *Assume that $\{\mu_1, A_1, \mathcal{V}_1\} \leq \{\mu_2, A_2, \mathcal{V}_2\}$ in the following sense:*

$$\forall \xi \in H^1(\Omega \setminus S, \mathbb{R}^3) \quad \int_{\partial S} A_1\xi \cdot \xi \mathrm{d}\mu_1 \leq \int_{\partial S} A_2\xi \cdot \xi \mathrm{d}\mu_2,$$
$$\textit{for q.e. } x \in \partial S,\ V_2(x) \subseteq V_1(x).$$

Then

$$T(\{\mu_1, A_1, \mathcal{V}_1\}, \mathbf{u}_1) \leq T(\{\mu_2, A_2, \mathcal{V}_2\}, \mathbf{u}_2).$$

Proof. The proof is a consequence of the energetic formulation of Stokes equations, introduced in (16). □

Remark 3.11 Since perfect slip boundary conditions correspond to

$$\mu_1 = 0, A_1 \equiv \mathrm{Id}, V_1(x) = \mathbb{R}^2,$$

and perfect adherence, to

$$\mu_2 = \infty|_{\partial S}, A_2 \equiv \mathrm{Id}, V_2(x) = \{0\},$$

the drag of an obstacle associated to perfect slip boundary conditions is lower than for perfect adherence.

Remark 3.12 Let us consider a riblet structure given by

$$\mu = 0, A \equiv \mathrm{Id}, V(x) = \mathbb{R}\xi(x),$$

where $\xi : \partial S \to S^1$. Clearly, the value of the drag associated to this micro-structure lays between the extremal ones. Nevertheless, the monotonicity is not strict since a good choice of the riblets ξ (they choice is depending on $\mathbf{u}_\infty$) can give the optimal drag associated to the perfect slip conditions. Of course, the same structure would not be optimal for a different $\mathbf{u}_\infty$.

This remarks justifies one of the main points of the paper, precisely that adding rugosity on an obstacle within a Stokes flow (in the sense of monotonicty of the micro structures given in Theorem 3.10), will not decrease the drag. In the best situation, when riblets are suitably chosen with respect to the flow, the drag will remain constant, otherwise it will increase. On the contrary, in the next section, we shall see from numerical experiments that for Navier-Stokes flows, adding rugosity may lead to the drag decrease.

4 Numerical computations

The purpose of this section is to give numerical evidence which justifies that adding suitable rugosity on the surface of an obstacle in a Navier-Stokes flow may decrease the drag.

In order to simplify the numerical computations, we fix the dimension of the space $N = 2$. In this case, the dimensions of the tangent spaces are 0 or 1, which can be simultaneously treated by a friction law, as follows.

We consider problem (1)-(5), where boundary conditions (4)-(5) take the form

$$\mathbf{u} \cdot \mathbf{n} = 0 \text{ on } \partial S, \tag{21}$$

$$[2\nu \mathbf{D}(\mathbf{u})\mathbf{n}]_{tan} + \beta \mathbf{u} = 0 \text{ on } \partial S. \tag{22}$$

Above, β is a nonnegative Borel function, possibly infinite valued, corresponding to the distribution of the friction coefficient on the boundary of the solid. Notice that if $\beta \equiv 0$, boundary conditions (21)-(22) correspond to perfect slip, and that perfect adherence is achieved formally by setting $\beta \equiv +\infty$.

For every such β and every weak solution $(\mathbf{u}, p)$ to problem (1)–(3), (21)–(22), we denote by $T(\beta, \mathbf{u})$ the corresponding drag, given by

$$T(\beta, \mathbf{u}) = 2\nu \int_{\Omega \setminus S} |\mathbf{D}(\mathbf{u})|^2 \, \mathrm{d}x + \int_{\partial S} \beta |\mathbf{u}|^2 \mathrm{d}\mathcal{H}^1.$$

In the numerical simulations, the domain Ω is the unit disk and the obstacle S is the disk of radius 0.1 centered at the origin. We assume that the fluid has a constant velocity $\mathbf{u}_\infty = (1, 0)$ on the exterior boundary $\partial\Omega$.

We apply a finite element method to solve problem (1)-(2), associated with boundary conditions (3),(21),(22). We use P_2 elements for the velocity and P_1 elements for the pressure. The fluid domain $\Omega \setminus S$ is discretized by a triangular mesh, which is obtained by an automatic

Mesh	Mesh size h_i	Number of triangles N_i	Numerical value of the drag	
			$\nu = 1$	$\nu = 10^{-2}$
M_0	0.0247922	5056	7.07255	0.240871
M_1	0.0123961	20224	7.07245	0.240847
M_2	0.00619805	80896	7.07244	0.240847

Table 1: Characteristics of the mesh and numerical value of the drag, with $\beta \equiv 1$, for $\nu = 1$ and $\nu = 10^{-2}$.

mesh generator, based on a Delaunay-Voronoi algorithm (see [8]). The stationary Navier-Stokes equations are solved by a classic fixed point iterative scheme and the incompressibility condition is treated by a Lagrange multiplier (see Girault and Raviart [9], [13]). Finally, the non penetration condition (21) is treated by penalization (see, for instance, Layton [16]).

4.1 Dependency of the numerical results with respect to the mesh

In order to estimate the influence of the mesh on the numerical value of the drag, we consider a family of meshes $\{M_0, M_1, M_2\}$ (see Figure 1). To describe the characteristics of these meshes, let us introduce some notation.

For $i = 0, 1, 2$, the mesh M_i is composed of N_i triangles, each of them being denoted by τ_i^j for $j = 1 \dots N_i$. To each mesh $M_i = \cup_{j=1}^{N_i} \tau_i^j$, we associate a mesh size h_i defined by

$$h_i = \left(\frac{1}{N_i} \sum_{j=1}^{N_i} |\tau_i^j| \right)^{1/2},$$

where $|\tau_i^j|$ stands for the area of triangle τ_i^j.

The meshes are built as follows. We start from a coarse mesh M_0, and for $i = 1, 2$, M_i is obtained by a refinement of mesh M_{i-1}. This refinement consists in a conformal splitting of each triangle of mesh M_{i-1}, into 4 triangles. Consequently, for $i = 1, 2$, $N_i = 4N_{i-1}$ and $h_i = \frac{1}{2} h_{i-1}$ (see Table 1).

To evaluate the influence of the mesh on the numerical results, we compute the drag associated to a constant friction coefficient $\beta \equiv 1$, using two different values for the viscosity: $\nu = 1$ and $\nu = 10^{-2}$. The numerical results of these computations are collected in Table 1. In the case of high viscosity ($\nu = 1$), we notice a global variation of order 10^{-4} of the drag computed on mesh M_0 and mesh M_2. Consequently, we will consider as relevant any drag reduction of order 10^{-3}, computed on grid M_2. In the case $\nu = 10^{-2}$, since the global variation of the numerical value of drag is of order 10^{-5}, a drag reduction of order 10^{-4} will be considered as relevant.

In the rest of this section, every numerical computation will be performed on the finest mesh M_2.

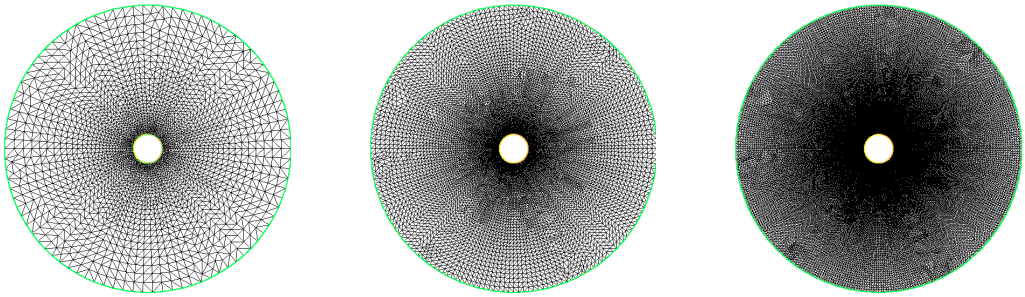

Figure 1: From left to right: meshes M_0, M_1, M_2. For $i = 1, 2$, mesh M_i is obtained by refining mesh M_{i-1}.

4.2 Minimization of the drag with respect to the friction coefficient β

In order to approach realistic situations, we fix a minimal value $+\infty > \beta_{min} > 0$ of the friction coefficient, and consider the following minimization problem:

$$\min \left\{ T(\beta, \mathbf{u}) \mid \beta \in L^2(\partial S),\ \beta \geq \beta_{min} \text{ a.e. on } \partial S \right\}. \tag{23}$$

Above, $\beta : \partial S \to \mathbb{R}_+$ is the friction distribution on the surface of the obstacle and satisfies $\beta(x) \geq \beta_{min}$ $\mathcal{H}^1$-a.e. on ∂S. To deal with this constrained optimization problem, we use a projective gradient method. We fix a stopping criterion ϵ, a constant step $h > 0$ and apply the following algorithm.

Gradient descent. Given a friction distribution β, satisfying the constraint $\beta \geq \beta_{min}$, we compute the gradient of T at β, in the sense of the Hilbert space $L^2(\partial S)$. We denote this function by $\nabla T(\beta)$. Next, we define the projected gradient $\mathcal{P}\nabla T(\beta) \in L^2(\partial S)$ by the following formula:

$$\mathcal{P}\nabla T(\beta) = \min \left(\nabla T(\beta), \frac{\beta - \beta_{min}}{h} \right). \tag{24}$$

While $\|\mathcal{P}\nabla T(\beta)\|_{L^2(\partial S)} > \epsilon$, we replace β by $\beta - h\mathcal{P}\nabla T(\beta)$ and iterate. Note that the projection step ensures that the constraint $\beta \geq \beta_{min}$ is preserved during the process.

The computation of the gradient of T with respect to β relies on the following result, which is proved in [2].

Proposition 4.1 *Let ν be large enough so that problem (1)–(3), (21)–(22) has a unique weak solution $(\mathbf{u}_\beta, p_\beta)$. Let $\mathcal{O}$ be the subset of $L^2(\partial S)$ defined by*

$$\mathcal{O} = \left\{ \beta \in L^2(\partial S) \mid \beta > 0 \text{ a.e. on } \partial S \right\}.$$

Then, the mapping

$$\beta \in \mathcal{O} \mapsto T(\beta) := T(\beta, \mathbf{u}_\beta) \in \mathbb{R}$$

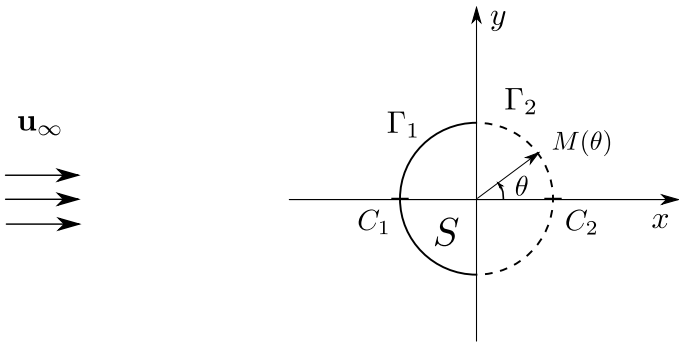

Figure 2: Notation and systems of coordinates used to describe the friction on the boundary of the solid.

is differentiable in $L^2(\partial S)$*. Moreover, its gradient can be represented by the following formula:*

$$\nabla T(\beta) = \left[(\mathbf{u}_\beta + \psi)\cdot \mathbf{u}_\beta\right]_{|\partial S}, \tag{25}$$

where $\psi \in H^1(\Omega \setminus S, \mathbb{R}^2)$ *is the unique solution to the adjoint system*

$$\begin{cases} -\text{div }(\sigma(\psi,p)) + (\nabla \mathbf{u})^T\psi - (\mathbf{u}\cdot\nabla)\psi = & 2(\mathbf{u}\cdot\nabla)\mathbf{u} \text{ in } \Omega\setminus S,\\ \text{div }\psi = & 0 \text{ in } \Omega\setminus S,\\ \psi = & 0 \text{ on } \partial\Omega,\\ \psi\cdot\mathbf{n} = & 0 \text{ on } \partial\mathcal{S},\\ [2\nu\mathbf{D}(\psi)\mathbf{n}]_{tan} + \beta\psi = & 0 \text{ on } \partial\mathcal{S}. \end{cases} \tag{26}$$

Below, we apply the gradient descent method introduced above, using the stopping criterion $\epsilon = 5\cdot 10^{-5}$ and the constant step $h = 2500$. We consider two values for the viscosity: $\nu = 1$ and $\nu = 10^{-2}$. In both cases, we start from a constant friction distribution $\beta \equiv 5$ and set the minimal value of the friction to $\beta_{min} = 1$.

To describe the distribution of the friction obtained at convergence of the algorithm, we identify each point $M \in \partial S$ by its angular coordinate $\theta \in \left[-\frac{\pi}{2}, \frac{3\pi}{2}\right]$, *i.e.* we set $M(\theta) = (0.1\cos\theta, 0.1\sin\theta)$. We introduce $\Gamma_1 = \left\{M(\theta) \mid \theta \in \left[\frac{\pi}{2}, \frac{3\pi}{2}\right]\right\}$, $\Gamma_2 = \left\{M(\theta) \mid \theta \in \left[-\frac{\pi}{2}, \frac{\pi}{2}\right]\right\}$, and we define $C_1 = M(\pi)$ and $C_2 = M(0)$ (see Figure 2). Moreover, given a friction distribution β, satisfying the constraint $\beta \geq 1 = \beta_{min}$, we say for $\mathcal{H}^1$-a.e. point M, that the constraint is saturated at $M \in \partial S$ provided that $\beta(M) = 1$.

4.2.1 High viscosity, $\nu = 1$

Table 2 gives the numerical value of the drag at each iteration, together with the L^2 norm of the projected gradient. We notice that the drag decreases significantly during the process, the final value being about 4.1% inferior to the initial one. At convergence, the constraint $\beta \geq 1$ is saturated at any points of ∂S, except at the central points C_1 and C_2 (see Figure 3). This leads to an irregular, non physical distribution of the friction. This can be explained by the fact that the exact velocity $\mathbf{u}$ of the fluid vanishes at points C_1 and C_2, by symmetry of

Iteration	Drag T	$\|\mathcal{P}\nabla T\|_{L^2(\partial S)}$
0	7.376	$123.9 \cdot 10^{-5}$
1	7.072	$7.7 \cdot 10^{-5}$
2	7.072	$3.1 \cdot 10^{-5}$
Case $\beta \equiv 1$	7.072	0

Table 2: Case $\nu = 1$. Numerical value of the drag and L^2 norm of the projected gradient, at each iteration of the gradient descent, and for the case $\beta \equiv 1$.

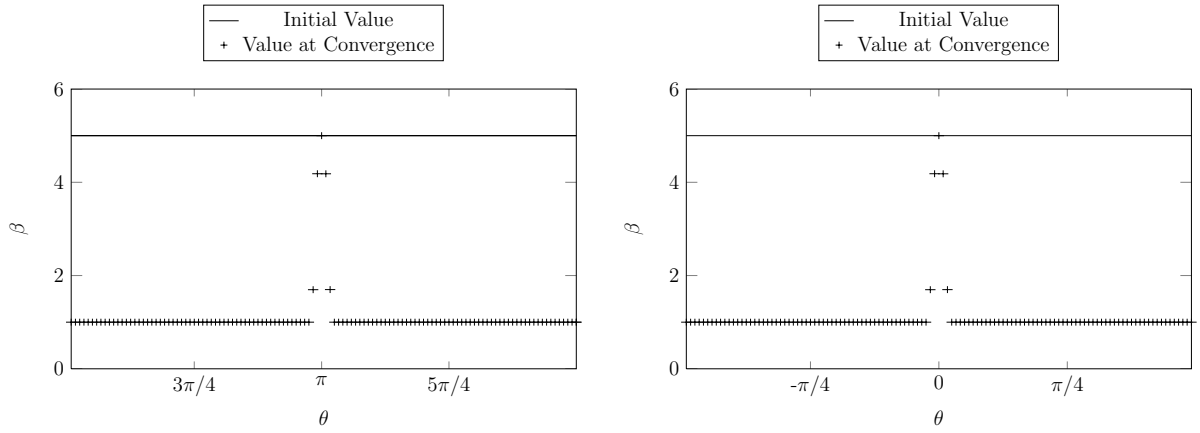

Figure 3: Case $\nu = 1$. Initial value of β and value at convergence, on Γ_1 (left) and Γ_2 (right), plotted against the angular coordinate θ.

the flow with respect to the axis $y = 0$. Consequently, formula (25) implies that the gradient of the drag is exactly zero at these points.

From a physical point of view, the tendancy to saturate globally the constraint $\beta \geq 1$ in order to minimize the drag, may be justified by the fact that for a viscosity $\nu = 1$, the Reynolds number associated with the flow is of order 1. As a result, the viscous effects are predominant, and as a consequence in that case, one should expect the drag to present a certain monotonicity with respect to the friction, as it happens when the inertial effects are neglected (see Theorem 3.10). From a numerical point of view, this is confirmed by the fact that the projected gradient of T, computed at $\beta \equiv 1$, is exactly zero.

4.2.2 Low viscosity, $\nu = 10^{-2}$

The results of the algorithm are presented in Table 3. At convergence, the value of the drag is about 6.4% inferior to its initial value. Moreover, it appears that the constant distribution $\beta \equiv 1$ is not optimal for this problem. This is confirmed by the fact that the norm of the projected gradient, computed at $\beta \equiv 1$, is significantly superior to the stopping criterion $\epsilon = 5 \cdot 10^{-5}$.

The distribution of the friction obtained at convergence is plotted in Figure 4. We observe that, contrary to the case $\nu = 1$, the constraint $\beta \geq 1$ is not saturated globally on ∂S. On

Iteration	Drag T	$\|\mathcal{P}\nabla T\|_{L^2(\partial S)}$
0	0.2569	$82.8 \cdot 10^{-5}$
1	0.2424	$30.5 \cdot 10^{-5}$
2	0.2409	$19.11 \cdot 10^{-5}$
3	0.2407	$12.9 \cdot 10^{-5}$
4	0.2406	$9.7 \cdot 10^{-5}$
5	0.2405	$7.5 \cdot 10^{-5}$
6	0.2405	$7.1 \cdot 10^{-5}$
7	0.2405	$5.3 \cdot 10^{-5}$
8	0.2405	$4.6 \cdot 10^{-5}$
Case $\beta \equiv 1$	0.2408	$70.2 \cdot 10^{-5}$

Table 3: Case $\nu = 10^{-2}$. Numerical value of the drag and L^2 norm of the projected gradient, at each iteration of the gradient descent, and for the case $\beta \equiv 1$.

the contrary, in a large vicinity of each point C_1 and C_2, the friction has *increased* during the process. This phenomenon is strongly marked on Γ_1, where the maximal value of the friction has doubled.

This example constitutes a numerical evidence that, for general viscous flows, smooth materials are not necessarily optimal for the problem of drag minimization. A combination of smooth parts, generating a small effective friction, and rough areas, associated with high friction coefficients, might lead to a better result.

5 Example of a complex rugosity effect

As the preceding numerical computations show, the effective boundary conditions obtained as a consequence of the micro-rugosity effect associated with perfect slip boundary conditions give *some* room to minimize the drag associated to a fixed obstacle, by acting on the "friction-driven" boundary conditions. This section is devoted to an example showing that with a similar construction, involving a slightly more complex control on the normal velocity (typically in-flow or out-flow conditions on *very* small regions), one can reach a significantly larger class of boundary conditions. Potentially, these boundary conditions could produce a stronger effect in the drag reduction.

A typical example in nature, that one may have in mind, is the shark skin. Modelling this highly complex rough surface is out of the mathematical purposes of the paper. Nevertheless, some features of this very singular surface can be loosely approached. Fine movements of the scales may drive a thin fluid layer through the open vertical spaces between the scales, so that from a mathematical point of view, one should consider, beside the "large" riblet surfaces of the scales, small vertical regions where the fluid flow can be oriented. This phenomenon is similar to synthetic jets, which consist in blowing and sucking fluid through thin holes on the surface, using electronic devices (see [17, Section 1.2.3]).

From a mathematical point of view, the "non penetration" condition $\mathbf{u} \cdot \mathbf{n} = 0$ on the

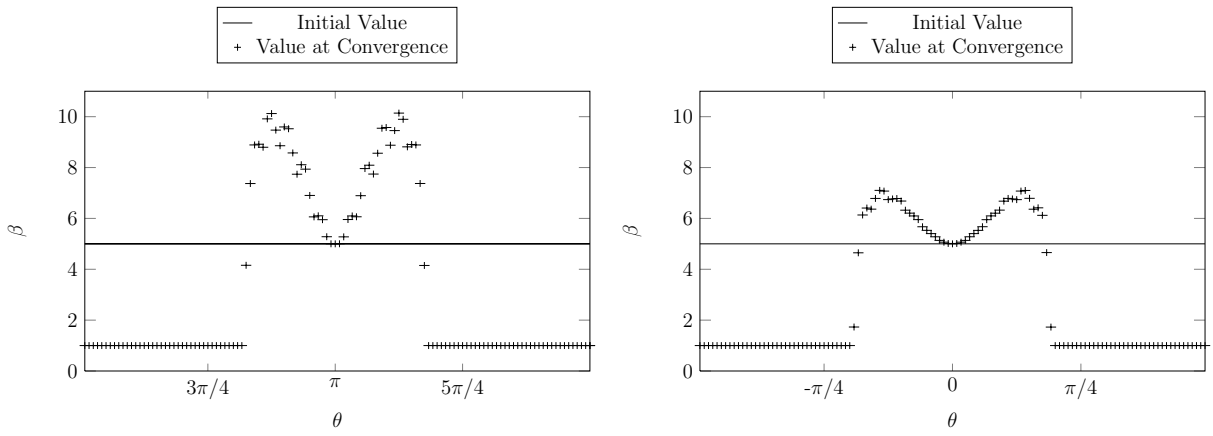

Figure 4: Case $\nu = 10^{-2}$. Initial value of β and value at convergence, on Γ_1 (left) and Γ_2 (right), plotted against the angular coordinate θ.

full boundary of the obstacle ∂S is then replaced by a *weak control* on the geometry of the surface of the obstacle where the normal velocity has a prescribed sign. In the example we give below, we consider a mixture of a *very small* region of in-flow complemented by a *large* region of perfect slip conditions on a rugous boundary. We prove that asymptotically, for a suitable distribution of the rugosity, the condition we obtain is significantly different from friction-driven. Precisely, we obtain an orientation of the flow on the full boundary of the obstacle. We treat this example only at an energetic level, formulated as a mathematical result describing the asymptotic behaviour of a sequence of Sobolev functions. Transporting this kind of result to understand the full behaviour of the solutions of Navier-Stokes equations would require more attention and should follow the same steps as in [4]. The full geometric control of the tangent vector spaces $V(x)$ is a challenging issue, even in absence of PDEs (e.g. [1]). However, it exceeds the purposes of the paper.

From the point of view of the drag minimization question, the main conclusion of this example is that the orientation of the flow can be seen as a new type of rugosity effect, out of the class of friction-driven boundary conditions, which effectively increases the space of controls $\mathcal{U}_\beta$ introduced in Section 3, opening new perspectives for the drag minimization.

The elementary piece of rugosity has the geometry of a (closed) prism $P(l, L, h) = [-\frac{l}{2}, \frac{l}{2}] \times \Delta_{h,L}$, where $\Delta_{h,L} := \{(x_2, x_3) : x_2 \in (0, L), x_3 \in (0, h - hx_2/L)\}$ is a right triangle of catheti of lengths h and L. Notice that the prism P has a vertical face V which is orthogonal to e_2 and two vertical faces orthogonal to e_1 (see Figure 5).

We construct sequence of open sets $\Omega_\varepsilon \subseteq (0,1)^3$

$$\Omega_\varepsilon = (0,1)^3 \setminus \bigcup_{i \in I_\varepsilon} \{(x_i^\varepsilon, y_i^\varepsilon, 0) + P(l_i^\varepsilon, L_i^\varepsilon, h_i^\varepsilon)\},$$

converging to the cube $\Omega = (0,1)^3$. The rugosity, denoted by σ_ε, is given by the *finite* union of prisms with random sizes $(l_i^\varepsilon, L_i^\varepsilon, h_i^\varepsilon)$, which are flattening, i.e. $\max_{i \in I_\varepsilon} h_i^\varepsilon \to 0$ as $\varepsilon \to 0$. For

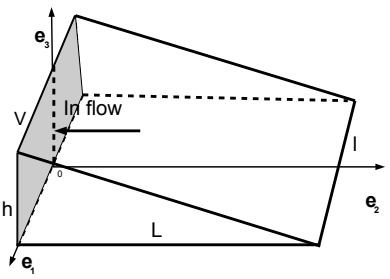

Figure 5: Shape of an elementary piece of rugosity $P(l, L, h)$.

every $i \in I_\varepsilon$, the rectangles

$$R_i^\varepsilon = (x_i^\varepsilon - \frac{l_i^\varepsilon}{2}, x_i^\varepsilon + \frac{l_i^\varepsilon}{2}) \times (y_i^\varepsilon, y_i^\varepsilon + L_i^\varepsilon)$$

are disjoint and contained in $[0,1]^2$. We assume the existence a constant C^ε depending on ε such that for every $i \in I^\varepsilon$ we have $h_i^\varepsilon = C^\varepsilon L_i^\varepsilon$. We introduce

$$\|\sigma_\varepsilon\| = \max_{i \in I_\varepsilon} L_i^\varepsilon + \left| [0,1]^2 \setminus \cup_{i \in I_\varepsilon} R_i^\varepsilon \right|.$$

For every set Ω_ε, the in-flow region consists in the union of the vertical faces (denoted V_ε) of the prisms orthogonal to e_2, while the perfect slip region is its complement $V_\varepsilon^c := \partial\Omega_\varepsilon \setminus V_\varepsilon$.

Proposition 5.1 *Assume that $\|\sigma_\varepsilon\| \to 0$. There exist $C^\varepsilon \to 0$ such that for every sequence of functions $\mathbf{u}_\varepsilon \in H^1(\Omega, \mathbb{R}^3)$ satisfying*

$$\mathbf{u}_\varepsilon \rightharpoonup \mathbf{u}$$

$$\mathbf{u}_\varepsilon \cdot \mathbf{n}_\varepsilon \leq 0 \text{ on } V_\varepsilon, \mathbf{u}_\varepsilon \cdot \mathbf{n}_\varepsilon = 0 \text{ on } V_\varepsilon^c$$

we have

$$\mathbf{u} \cdot e_3 = 0 \text{ on } (0,1)^2 \times \{0\}, \quad \mathbf{u} \cdot e_2 \leq 0 \text{ on } (0,1)^2 \times \{0\}.$$

Proof. First, we prove that for every $C^\varepsilon \to 0$, the non penetration condition $\mathbf{u} \cdot e_3 = 0$ on $(0,1)^2 \times \{0\}$ is achieved. In a second step, a special choice for C^ε will insure the orientation of the flow, $\mathbf{u} \cdot e_2 \leq 0$ on $(0,1)^2 \times \{0\}$.

For every $(x,y) \in (0,1)^2$, we denote $\varphi_\varepsilon(x,y) = \sup\{z \in [0,1) : (x,y,z) \in \partial\Omega_\varepsilon\}$. For almost every $(x,y) \in (0,1)^2$, we denote $\mathbf{n}_\varepsilon = (-\nabla\varphi_\varepsilon, 1)/\|(-\nabla\varphi_\varepsilon, 1)\|$. Assume that $C^\varepsilon \to 0$, thus $\|\mathbf{n}_\varepsilon - e_3\|_{L^\infty} \to 0$.

We have for almost every $(x,y) \in (0,1)^2$,

$$\mathbf{u}_\varepsilon(x,y,\varphi_\varepsilon(x,y)) - \mathbf{u}_\varepsilon(x,y,0) = \int_0^{\varphi_\varepsilon(x,y)} \frac{\partial \mathbf{u}_\varepsilon}{\partial z}(x,y,z) \mathrm{d}z.$$

Multiplying by the normal field $\mathbf{n}_\varepsilon(x,y,\varphi_\varepsilon(x,y))$ (simply denoted in the sequel $\mathbf{n}_\varepsilon$), we obtain

$$\mathbf{u}_\varepsilon(x,y,\varphi_\varepsilon(x,y))\cdot\mathbf{n}_\varepsilon-\mathbf{u}_\varepsilon(x,y,0)\cdot\mathbf{n}_\varepsilon=\mathbf{n}_\varepsilon\cdot\int_0^{\varphi_\varepsilon(x,y)}\frac{\partial\mathbf{u}_\varepsilon}{\partial z}(x,y,z)\mathrm{d}z,$$

which yields

$$|\mathbf{u}_\varepsilon(x,y,0)\cdot e_3|\le|\mathbf{u}_\varepsilon(x,y,0)|\|\mathbf{n}_\varepsilon-e_3\|_{L^\infty}+(C^\varepsilon\sigma_\varepsilon)^{\frac12}\left(\int_0^{\varphi_\varepsilon(x,y)}|\frac{\partial\mathbf{u}_\varepsilon}{\partial z}(x,y,z)|^2\mathrm{d}z\right)^{1/2}.$$

Consequently,

$$\int_{(0,1)^2\times\{0\}}|\mathbf{u}_\varepsilon(x,y,0)\cdot e_3|^2\mathrm{d}x\mathrm{d}y\le2\|\mathbf{n}_\varepsilon-e_3\|_{L^\infty}^2\int_{(0,1^2)}|\mathbf{u}_\varepsilon(x,y,0)|^2\mathrm{d}x\mathrm{d}y+2C^\varepsilon\sigma_\varepsilon\left\|\frac{\partial\mathbf{u}_\varepsilon}{\partial z}\right\|_{L^2(\Omega)}^2.$$

Letting $\varepsilon\to0$, using the continuity of the trace $H^1(\Omega)\to L^2((0,1)^2\times\{0\})$, the non penetration condition follows on $(0,1)^2\times\{0\}$.

In order to prove that the orientation of the flow is achieved for a special choice of C^ε, we use a classical way to estimate the vanishing region of a scalar Sobolev function in terms of capacity (see for instance [3, Section 4.6]). In a first step, let us assume that $C^\varepsilon=C$ is a constant independent on ε. For every ε, we shall give an estimate of the local capacity of the set V_ε. By construction of the rugous domains, there exists a constant δ depending only on C, such that for every $\varepsilon>0$ with $\sigma_\varepsilon<\frac{\pi r^2}{2}<\frac{\pi}{8}$, for every point $\mathbf{x}\in(0,1)\times(0,1)\times\{0\}$ we have

$$\mathcal{H}^2(V_\varepsilon\cap B_r(\mathbf{x}))\ge\delta r^2.$$

Let us consider $P:\mathbb{R}^3\to\mathcal{H}$, the orthogonal projection on the plane $\mathcal{H}=\{\mathbf{x}\in\mathbb{R}^3:x_2+x_3=1\}$. There exists a constant δ' such that

$$\mathcal{H}^2(P(V_\varepsilon)\cap B_r(P(\mathbf{x})))\ge\delta' r^2.$$

Relying on the behaviour of capacity on Steiner symmetrization (a first symmetrization with respect to the plane, followed by a second symmetrization with respect to an axis orthogonal to the plane), there exists a constant δ'' such that

$$\mathrm{cap}(V_\varepsilon\cap B_r(\mathbf{x}),B_r(2\mathbf{x}))\ge\delta''\,\mathrm{cap}(B_r(\mathbf{x}),B_r(2\mathbf{x})).$$

This capacity inequality provides a sufficient condition (see for instance [3, Example 4.6.3]), to get that the condition $\mathbf{u}_\varepsilon\cdot\mathbf{n}_\varepsilon\le0$ on V_ε transforms into the limit in $(\mathbf{u}\cdot e_2)^+=0$ on $[0,1]\times[0,1]\times\{0\}$. By a diagonal procedure, relying on the metrizability of the Γ-convergence, the same property holds for a suitable sequence $C^\varepsilon\to0$. □

Remark 5.2 If C_ε does not converge to zero, the rugosity effect produced by the non vertical face of the elementary prism leads to a global in-flow condition $\mathbf{u}\cdot e_3\ge0$ on the flat boundary. This is a consequence of the capacity density argument. As $C_\varepsilon\to0$, the asymptotic effect of this face leads to the non penetration condition $\mathbf{u}\cdot e_3=0$. The choice of the values of C_ε depends on σ_ε, but cannot be computed explicitly in a non periodical geometry. We also notice that the vertical faces of the prisms parallel to e_2, may or may not produce a secondary rugosity effect, which would lead to $\mathbf{u}\cdot e_1=0$, depending on their distribution. If this secondary rugosity effect holds, clearly the macroscopic condition $\mathbf{u}\cdot e_2\le0$ obtained in Proposition 5.1 is strengthen, the flow being oriented onto the e_2 axis.

Acknowledgments

This work is part of the project ANR-09-BLAN-0037 *Geometric analysis of optimal shapes (GAOS)* financed by the French Agence Nationale de la Recherche (ANR).

References

[1] P. Birtea and D. Comănescu, *Geometrical Dissipation for Dynamical Systems*, Comm. Math. Phys., 316 (2012), pp. 375–394.

[2] M. Bonnivard, *Influence des perturbations géoémétriques des domaines sur les solutions d'équations aux dérivées partielles*, PhD Thesis, Université de Grenoble, HAL, http://hal.archives-ouvertes.fr/tel-00555121, 2010.

[3] D. Bucur and G. Buttazzo, *Variational methods in shape optimization problems*, Progress in Nonlinear Differential Equations and their Applications, 65, Birkhäuser Boston Inc., Boston, MA, 2005.

[4] D. Bucur, E. Feireisl, and Š. Nečasová, *Boundary behavior of viscous fluids: Influence of wall roughness and friction-driven boundary conditions*, Arch. Ration. Mech. Anal., 197 (2010), pp. 117–138.

[5] J. Casado-Díaz, M. Luna-Laynez, and F. J. Suárez-Grau, *Asymptotic behavior of a viscous fluid with slip boundary conditions on a slightly rough wall*, Math. Models Methods Appl. Sci., 20 (2010), pp. 121–156.

[6] G. Dal Maso, *An introduction to* Γ*-convergence*, Progress in Nonlinear Differential Equations and their Applications, 8, Birkhäuser Boston Inc., Boston, MA, 1993.

[7] Z. Gao, Y. Ma, and H. Zhuang, *Drag minimization for Navier-Stokes flow*, Numer. Methods Partial Differential Equations, 25 (2009), pp. 1149–1166.

[8] P. L. George, *Automatic mesh generation and finite element computation*, in Handbook of numerical analysis, Vol. IV, Handb. Numer. Anal., IV, North-Holland, Amsterdam, 1996, pp. 69–190.

[9] V. Girault and P.-A. Raviart, *Finite element methods for Navier-Stokes equations*, vol. 5 of Springer Series in Computational Mathematics, Springer-Verlag, Berlin, 1986. Theory and algorithms.

[10] M. D. Gunzburger, H. Kim, and S. Manservisi, *On a shape control problem for the stationary Navier-Stokes equations*, M2AN Math. Model. Numer. Anal., 34 (2000), pp. 1233–1258.

[11] L. I. Hedberg, *Spectral synthesis in Sobolev spaces, and uniqueness of solutions of the Dirichlet problem*, Acta Math., 147 (1981), pp. 237–264.

[12] A. Henrot and M. Pierre, *Variation et Optimisation de Formes*, Mathématiques et Applications, Springer-Verlag, Berlin, 2005.

[13] K. Ito and K. Kunisch, *Lagrange multiplier approach to variational problems and applications*, vol. 15 of Advances in Design and Control, Society for Industrial and Applied Mathematics (SIAM), Philadelphia, PA, 2008.

[14] W. Jäger and A. Mikelić, *Couette flows over a rough boundary and drag reduction*, Comm. Math. Phys., 232 (2003), pp. 429–455.

[15] E. Lauga, M. Brenner, and H. Stone, *Microfluidics: The no-slip boundary condition*, Handbook of Experimental Fluid Dynamics, Editors J. Foss, C. Tropea and A. Yarin, Springer, New-York, 2007.

[16] W. Layton, *Weak imposition of "no-slip" conditions in finite element methods*, Comput. Math. Appl., 38 (1999), pp. 129–142.

[17] B. Mohammadi and O. Pironneau, *Applied shape optimization for fluids*, Numerical Mathematics and Scientific Computation, Oxford University Press, Oxford, second ed., 2010.

[18] J. Nečas, *On domains of type n*, Czechoslovak Math. J., 12 (87) (1962), pp. 274–287.

[19] P. I. Plotnikov and J. Sokolowski, *Shape derivative of drag functional*, SIAM J. Control Optim., 48 (2010), pp. 4680–4706.

[20] N. V. Priezjev, A. A. Darhuber, and S. M. Troian, *Slip behavior in liquid films on surfaces of patterned wettability: Comparison between continuum and molecular dynamics simulations*, Phys. Rev. E, 71 (2005), p. 041608.

[21] T. Qian, X.-P. Wang, and P. Sheng, *Hydrodynamic slip boundary condition at chemically patterned surfaces: A continuum deduction from molecular dynamics*, Phys. Rev. E, 72 (2005), p. 022501.

[22] J. Simon, *Domain variation for drag in Stokes flow*, in Control theory of distributed parameter systems and applications (Shanghai, 1990), vol. 159 of Lecture Notes in Control and Inform. Sci., Springer, Berlin, 1991, pp. 28–42.

[23] S. Vogel, *Life in moving of fluids; the physical biology of flow*, Numerical Mathematics and Scientific Computation, Princeton University Press, 1994. Princeton, N.J.

[24] W. P. Ziemer, *Weakly differentiable functions*, vol. 120 of Graduate Texts in Mathematics, Springer-Verlag, New York, 1989. Sobolev spaces and functions of bounded variation.

Matthieu Bonnivard: Univ. Paris Diderot, Sorbonne Paris Cité
Laboratoire Jacques-Louis Lions, UMR 7598, UPMC, CNRS
F-75205 Paris, France
bonnivard@ljll.univ-paris-diderot.fr

Dorin Bucur: Laboratoire de Mathématiques (LAMA, UMR 5127), Université de Savoie
Campus Scientifique, 73376 Le Bourget-Du-Lac, France
dorin.bucur@univ-savoie.fr